

# 3-D CFD ANALYSIS ON EFFECT OF HUB-TO-TIP RATIO ON PERFORMANCE OF IMPULSE TURBINE FOR WAVE ENERGY CONVERSION

by

**Ajit THAKKER and Mohammed A. ELHEMRY**

Original scientific paper

UDC: 532.592:621.438.1:519.876.5

BIBLID: 0354-9836, 11 (2007), 4, 157-170

*This paper deals with the computational fluid dynamics analysis on effect of hub-to-tip ratio on performance of 0.6 m impulse turbine for wave energy conversion. Experiments have been conducted on the 0.6 m impulse turbine with 0.6 hub-to-tip ratio to validate the present computational fluid dynamics method and to analyze the aerodynamics in rotor and guide vanes, which demonstrates the necessity to improve the blade and guide vanes shape. Computational fluid dynamics analysis has been made on impulse turbine with different hub-to-tip ratio for various flow coefficients. The present computational fluid dynamics model can predict the experimental values with reasonable degree of accuracy. It also showed that the downstream guide vanes make considerable total pressure drop thus reducing the performance of the turbine. The computational fluid dynamics results showed that at the designed flow coefficient of 1.0 the turbine with 0.5 hub-to-tip ratio has better performance compared to 0.55 and 0.6 hub-to-tip ratio turbine.*

Key words: wave energy, impulse turbine, computational fluid dynamics, hub-to-tip ratio

## Introduction

The current rate of worldwide energy use is unsustainable, mainly due to the dependence on the use of fossil fuels as the primary sources of available energy. Based on the current usage trends of the fossil fuels it is predicted that current quantities will be exhausted in approximately 200 years. The current usage of available resources is indicating that in a matter of years, the world will face a period of shortages, escalating prices and increasing international tensions, as developing countries demand their share of a rapidly dwindling resource. Throughout the years, several concepts were developed and investigated: the Salter Duck, Cockerell raft, the "SEA clam", and oscillating water column (OWC) devices. These wave energy devices are either shore mounted or offshore. Shore-mounted devices are fixed and easier to design but harness less energy from shallow waters. Shore based converters are generally oscillating water column [1]. Shore-mounted OWC converters have been erected in Norway, UK (Isle of Islay) and

Portugal (Island of Pico). Offshore converters can be either fixed seabed or floating and are meant for the height wave power density of the offshore sea. The various offshore devices use different energy conversion chains; the wave power can be captured by hydraulic systems, water turbines or air turbines, via a wave to pneumatic converter. These devices include the circular Clam, Salter's Duckt, and the floating OWC. Examples of the floating OWC are the "whale" and the backward bent duct buoy (BBDB), both originating from Japan. One of the most promising techniques for harnessing wave energy is the OWC. OWC based wave energy plants convert energy into low-pressure pneumatic power in the form of bidirectional airflow. Air turbines which are capable of rotating unidirectional in a bidirectional air flows, otherwise also known as self-rectifying air turbines are used to extract mechanical shaft power, which is further converted into electrical power by a generator. Different type of impulse turbine have been proposed over the year, but generally their performance has not been investigated except may in the case of McCormick turbine whose efficiency found to be rather low. The Wells turbine, introduced by Dr. A. A. Wells in 1976 was the first choice for all OWC based wave energy plants, which were built in Norway, Japan, Scotland, India, and China. There are many reports, which described the performance of the Wells turbine both at starting and running conditions [2-4]. According to these results, the Wells turbine has inherent disadvantage: narrow range of flow rate at which it operates at useful efficiencies due to stall problem, poor starting characteristics, high-speed operation and consequent noise and high axial thrust. Setoguchi *et al.* [5-12] developed an impulse turbine with self-pitching controlled guide vanes and subsequently with self-pitching linked guide vanes to overcome the drawbacks of the Wells turbine. Numbers of studies were conducted on impulse turbine with self-pitch controlled guide vanes over a period of time. The turbine has a rotor with impulse blades. There two sets of guide vanes on either side of the rotor. The guide vanes are pivoted and are free to rotate between two preset angles determined by mechanical stops. Whenever the airflow change the direction, the guide vanes flip under the action of aerodynamic moments acting on them, and take up the right orientations (that is, upstream guide vanes acting as nozzle cascade and downstream guide vanes acting as a diffuser cascade) for efficient operation. Later impulse turbine with self-pitching guide vanes were proposed, this type have the same design as the previous impulse turbine with controlled guide vanes except that the every vane on one side of the rotor is connected by a link outside of the rotor. That is, any pair of vanes on either side of the rotor is constrained to rotate together. This design delivers useful efficiencies over a wide range of flow rates, has very good starting characteristics and low operating speed. These characteristics have been put up with field trial. A 1.0-m diameter turbine of this type was designed, fabricated and is being operated by National Institute of Ocean Technology at Vizhinjam, a site near Thiruvananthapuram which is a city on the west coast of India. Notwithstanding the superior characteristics of the impulse turbine with self-pitch controlled guide vanes, certain disadvantages are imposed by such variable geometry design. The guide vanes pitch at the wave frequency calling for a robust mechanical design to withstand a large number of oscillation cycles per day. The moving parts lead to maintenance and operating life problems and more cost. If a fixed guide vane were provided instead, it was felt that these problems would be mitigated even though the performance

may be poorer. With this in view, model test were conducted to determine the characteristics of fixed guide vane impulse turbine. The results were encouraging and more test were conducted to optimise various parameters of the turbine. There are few reports presented on the numerical analysis on impulse turbine and Wells turbine for wave energy conversion application. Kim *et al.* [13] have investigated an optimal installation angle of the impulse turbine by numerical analysis. In order to achieve improvement in the performance of the impulse turbine, the effect of 3-D guide vanes has been investigated experimentally by testing a model under unsteady bidirectional flow conditions [14] and found that the performance of the turbine with 3-D guide vanes are superior to those with 2-D guide vanes. The effect of tip clearance on the performance of Wells turbine has been investigated experimentally by few authors [15-17] and found that the turbine is very sensitive to tip clearance when compared to a conventional turbine. On the other hand the effect of tip clearance on performance of impulse turbine with fixed guide vanes have been investigated by Thakker *et al.* [18].

Based on the re-review of the state-of-the-art of the wave energy technology, it was found that there is a scope for enhancing the performance of impulse turbine with fixed guide vanes by conducting further design analysis and detailed flow investigation. The objective of this paper is to present the computed effect of hub-to-tip ratio (H/T) on performance of 0.6 m diameter impulse turbine with fixed guide vanes for wave energy conversion using 3-D computational fluid dynamics (CFD) analysis as a tool under steady flow condition. Aerodynamic studies have been made experimentally and computationally to understand the pressure losses in the rotor and guide vanes.

### Experimental analysis

A schematic layout of the experimental set-up of Wave Energy Research Team at University of Limerick is shown in fig. 1. It consists of a bell-mouth entry, test section, drive and transmission section, a plenum chamber with honeycomb section, a calibrated nozzle, and a centrifugal fan.

Air is drawn into the bell-mouth shaped open end; it passes through the turbine and then enters the plenum chamber. In the chamber, the flow is conditioned and all swirls/vortices are removed prior to passing through a calibrated nozzle and finally exhausting at the fan outlet. A valve at fan exit controls the flow rate. Details of the test rig calibration can be found in [19]. The turbine test section had an inter-

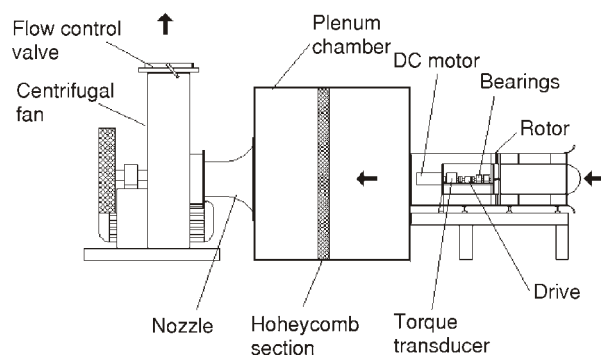


**Figure 1. Schematic diagram of the test rig at University of Limerick**

nal diameter of 600 mm and fabricated rotor had a diameter of 598 mm, leaving tip clearance of 1 mm. The hub diameter selected as 358.8 mm, providing H/T of 0.6. The specification of the turbine is listed in tab. 1. The geometry has been arrived based on the investigations by Setoguchi *et al.* [20], who conducted large number of experiments on impulse turbine with different pitch chord ratio, blade profile and H/T of 0.7, 0.8, and 0.85. They also concluded that the most favourable pitch chord ratio is 0.5. The turbine was mounted on a shaft in a cylindrical annular duct, with a blade tip clearance of 1 mm. The shaft is coupled to motor/generator via a torque meter. The two rows of guide vanes (3-D) were mounted on the upstream and downstream hubs of the rig. The turbine was tested by keeping a constant axial air velocity of 8.49 m/s. Data was collected by varying the rotational speed of the turbine from 1250 rpm to 125 rpm by loading the generator, thus giving a flow coefficient in the range of 0.27 to 2.7. The apparatus is fully equipped with instrumentation for measuring the essential parameters like torque, speed, and pressure. A vibrometer torque transducer (Model TM 204-208) measures the torque and speed. The mechanical losses due to bearing friction and windage losses were tested before commissioning the rig and a mean torque curve was deduced to correct the measured torque reading. Measurement of pressure was made by means of pneumatic pressure probes. A miniaturized five-hole probe was used for aerodynamic measurements at 40 mm ahead of inlet guide vane (IGV) inlet, 10 mm behind IGV, 10 mm behind the turbine, and 80 mm behind downstream guide vane (DGV). The probe was mounted on traverse mechanism fixed to the turbine outer casing of the test rig. Furness Control micro-manometer (Model FC012, Furness Controls Ltd, UK) through a 60 channel scanning box (Model FCS421, Furness Controls Ltd, UK) with a least count of 0.01 mm of water column were used to read the pressure data. Pressure measurements were carried out at 11 equi-spaced radial locations. The probe data obtained was reduced using the calibration

**Table 1. Specification of the turbine**

<i>Blade profile: H/T</i>	0.5	0.55	0.6
Number of blades	30	30	30
Tip diameter [mm]	598.0	598.0	598.0
Chord length [mm]	93.93	97.06	100.20
Blade pitch [mm]	46.97	48.53	50.10
Blade inlet angle	60°	60°	60°
<i>Guide vanes profile:</i>			
Pitch [mm]	54.19	56.00	57.81
Chord length [mm]	123.16	127.27	131.38
Number of guide vanes	26	26	26
Guide vanes angle	30°	30°	30°

charts to evaluate all necessary parameters, including the flow rates. The Reynolds number based on the blade chord length was  $0.74 \cdot 10^5$  at peak efficiency.

The overall performance of the turbine was evaluated by the turbine angular velocity  $\omega$ , torque generated  $T$ , flow rate  $Q$ , and total pressure drop  $\delta p$  across the rotor. The results are expressed in the form of torque coefficient  $C_T$ , input power coefficient  $C_A$ , and efficiency  $\eta$  in terms of flow coefficient  $\phi$ . The definitions are:

$$C_T = \frac{T}{\frac{\rho(v_a^2 + U_R^2) b l_r z r_R}{2}} \quad (1)$$

$$C_A = \frac{\delta p Q}{\rho(V_a^2 + U_R^2) b l_r z v_a} \quad (2)$$

$$\phi = \frac{v_a^2}{U_R} \quad (3)$$

$$\eta = \frac{T\omega}{\delta p Q} = \frac{C_T}{C_A \phi} \quad (4)$$

### Design of 0.6 m impulse turbine

Calculations were made to define the entire blade and guide vane geometry parameters. A worksheet was created in Microsoft Excel to define the complete blade and guide vane geometry profile data for 0.6 m impulse turbine by giving, the required initial design constraints, such as rotor diameter, H/T, guide vane inlet and outlet angles, number of blades and guide vanes, all the other parameters are calculated automatically. 2-D drawing of turbine blade and guide vanes were produced using AutoCAD to validate this design data. Following this validation, a 3-D solid model was generated using CAD package Pro-Engineer v2.0.

### Numerical method and calculation

GAMBIT 2.0 and FLUENT V6 were used for meshing and analyzing the problem, respectively. The computational grid is visualized in fig. 2, where only the grid lines attached to the surfaces are shown. Here, the resolution of all the bound-

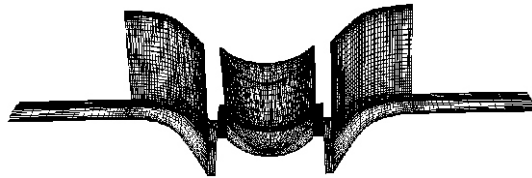
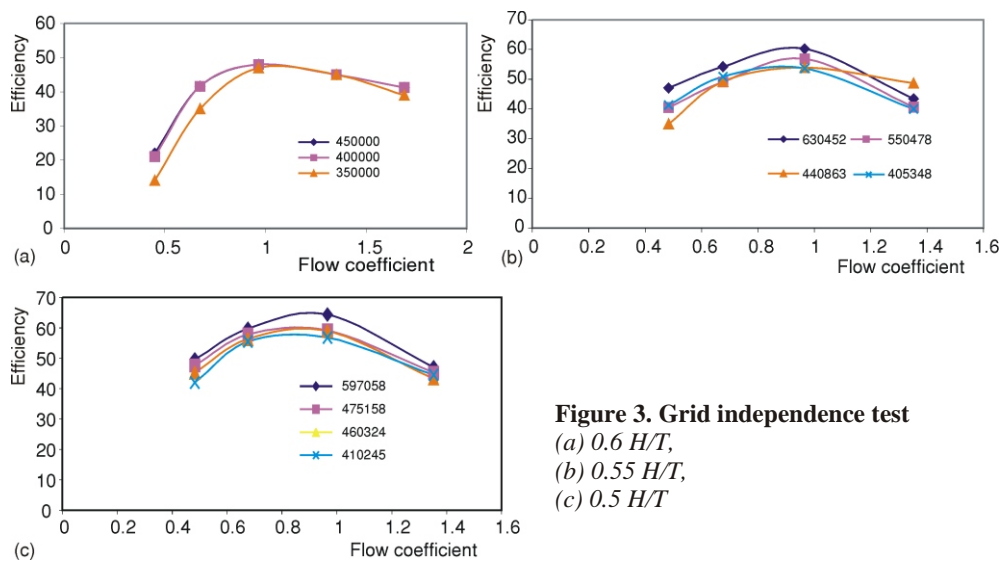


Figure 2. Computational grid

ary layers is visible. The grids are clustered near the hub, casing, and tip to give appropriate  $y^+$  values. Also the matter of grid independence has been taken a serious consideration in the presents CFD analysis. By employing finite number of grid points distributed over the flow filed the numerical results will be effected by the grid parameters, grid structure, grid distribution, and number of grid. In order to examine the grid dependency on numerical accuracy a grid independence test has been carried out on the computational domain. The performance tests of the turbine for various cases are shown in fig. 3a-c. A total num-



**Figure 3. Grid independence test**  
 (a) 0.6 H/T,  
 (b) 0.55 H/T,  
 (c) 0.5 H/T

ber of 400,000, 500,000, and 600,000 grid cells are used for 0.5, 0.55, and 0.6 H/T, respectively. It was necessary to set up three fluid zones using mixing plane technique. Three zones are the upstream guide vane, the rotor and the downstream guide vane. The fluid at rotor is defined as a moving reference frame with the angular speed equivalent to that of the blade. Inflow is set as mass flow inlet, outflow is set as pressure outlet and periodic walls are set as transitional to allow cascade effect on blade and guide vane to be simulated. The essential idea behind the mixing plane concept is that each fluid zone is solved as a steady-state problem. At some prescribed iteration interval, the flow data at the mixing plane interface are averaged in the circumferential direction on both the stator outlet and the rotor inlet boundaries FLUENT manual [21]. The code implementation uses area-weighted averages. By performing circumferential averages at specified radial or axial stations, "profiles" of flow properties can be defined. These profiles, which will be functions of axial coordinate, are then used to update boundary conditions along the two zones of the mixing plane interface. The flow is set as fully turbulent.

## Results and discussion

### Validation of numerical procedure

In order to validate the present numerical model, the computed and measured values of input coefficient, torque coefficient and efficiency have been compared at various flow coefficients. From the input coefficient prediction in fig. 4a, the computed value gives higher input coefficient at high flow coefficient but generally the same shape as the experimental measured values. A good agreement between computed and experimental measured torque coefficient values are shown in fig. 4b, these indicate the 3-D flow and torque delivered by the turbine is correctly predicted by the CFD. From fig. 4c, the efficiency predicted by CFD is in excellent agreement with the experimental measured results, for the entire flow coefficient except at very low coefficients.

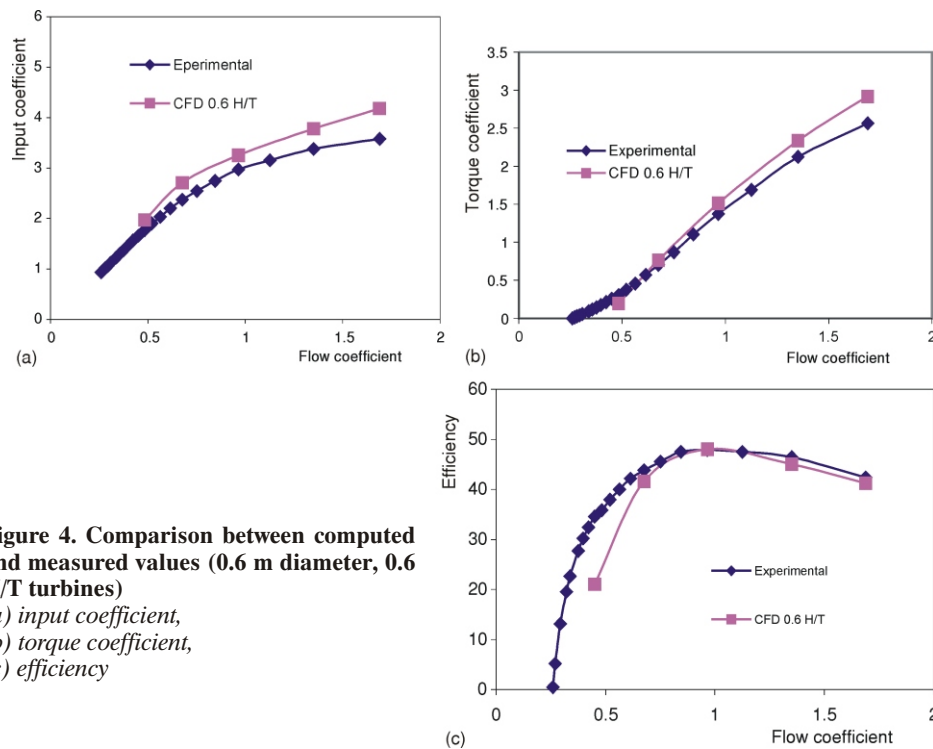


**Figure 4. Comparison between computed and measured values (0.6 m diameter, 0.6 H/T turbines)**

(a) input coefficient,  
(b) torque coefficient,  
(c) efficiency

### Measured guide vane losses on performance of 0.6 m impulse turbine

Experiments have been conducted to investigate rotor and guide vanes losses on performance of the impulse turbine [14]. Also, aerodynamic measurements have been

made at various radius ratios,  $R$  ( $R = r/r_t$ ), where  $r$  is the radius where measurement has been made and  $r_t$  is the tip radius) to analyze the flow and to measure the losses at various stations like outlet of inlet guide vane, behind rotor, and behind downstream guide vane. Figures 5a-e, show the variation of pressure loss coefficient at various stations from hub-to-tip region for the flow coefficients  $\phi = 0.45, 0.67, 1.00, 1.35$ , and  $1.68$ , respectively. The total pressure loss coefficient has been defined as:

$$C_{Pt} = \frac{P_{oi}}{P_{oi}} \frac{P_o}{P_{si}} \quad (5)$$

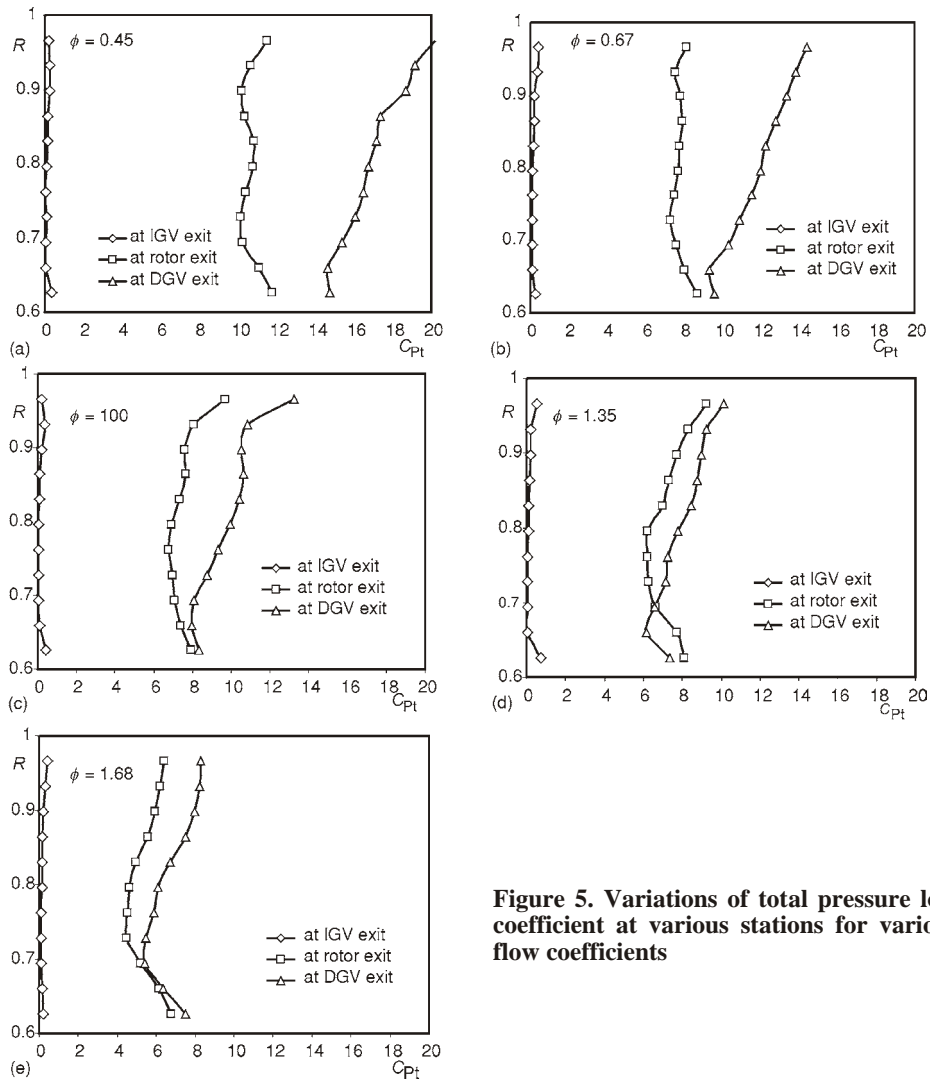
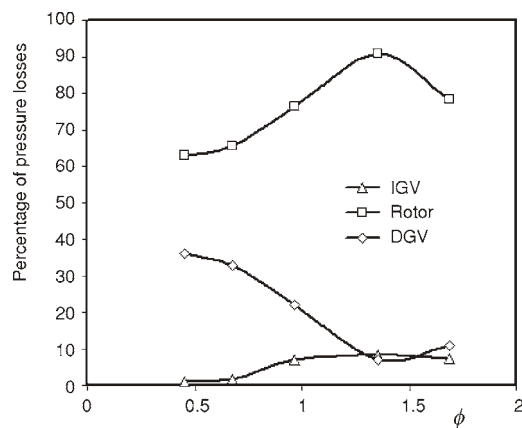


**Figure 5. Variations of total pressure loss coefficient at various stations for various flow coefficients**



where  $P$  is the pressure and the subscripts i, o, and s denotes inlet conditions, total conditions, and static conditions, respectively. The pressure drop due to inlet guide vanes is almost negligible and uniform from hub-to-tip in all the flow coefficients, as the flow is steady and two-dimensional. From the figs. 5a-c, it can be seen that the pressure drop across the turbine is nearly uniform from hub-to-tip and its mean value seems very high at  $\phi = 0.45$  and reducing drastically up to  $\phi = 1.0$ . Beyond the value of  $\phi = 1.0$ , fig. 5d-e, rotor pressure losses are more in the tip region from  $R = 0.8$  to  $1.0$  due to wake effects and tip clearance leakage vortex. It is very clearly seen from the figure that the pressure drop due to downstream guide vanes is very high with reference to the pressure drop curve of rotor, especially at the flow coefficients  $\phi = 0.45, 0.67$ , and  $1.0$ , figs. 5a-c. It can also be noted that the pressure drop at DGV follows the same trend of rotor-loss-curve above  $\phi = 1.0$ . From the above discussion, it is clear that the DGV plays important role for considerable reduction in efficiency of the turbine and hence the guide vanes have been designed according to free vortex theory. Computational analysis has been made to calculate the advantage of using twisted guide vanes on performance of the turbine and also to understand the change in flow behaviour due to effect of twisted guide vanes, and the results are presented in the next section. The values of  $C_{Pt}$  at various stations are averaged circumferentially from hub-to-tip for various flow coefficients and plotted in fig. 6. The figure shows that the total pressure drops about 40% in the DGV at lower flow coefficients and about 10% at higher flow coefficients. It can also be observed that there is a straight correlation between pressure loss coefficients in the rotor and the DGV rather than IGV. It expounds the need of improvement in aerodynamic design of DGV to enhance the performance of turbine for wide range of flow coefficient.

**Figure 6. Variation of percentage of total pressure loss coefficient with flow coefficient**



*Computed effect of H/T on the performance of the impulse turbine*

Figures 7a-c shows the variations of  $C_T$ ,  $C_A$ , and efficiency of 0.6 m impulse turbine with 0.5, 0.55, and 0.6 H/T, respectively, with respect to flow coefficients. Figure

7a, shows the improvement in torque developed by the turbine with 0.5 H/T for the full range of flow coefficient as compared to 0.55 and 0.6 H/T turbine. In particular the improvement is well noticed above the flow coefficient of 1.0. At the same time, while considering the pressure drop across the turbine, the drop in pressure due to 0.5 H/T turbine is slightly higher when compared to 0.55 and 0.6 H/T turbine. Also for 0.5 H/T turbine, higher torque generated, thus resulting into higher efficiency for full range of flow coefficient. The efficiency of the turbine with 0.5, 0.55, and 0.6 H/T is shown in fig. 7c. The figure shows the turbine efficiency has improved considerably due to 0.5 H/T throughout the range of flow coefficients. The maximum improvement in efficiency about 7.1% is observed at the designed condition of flow coefficient 1.0. Furthermore, in the off-design conditions, the turbine efficiency of 0.5 H/T is greater than that of 0.55 and 0.6 H/T.

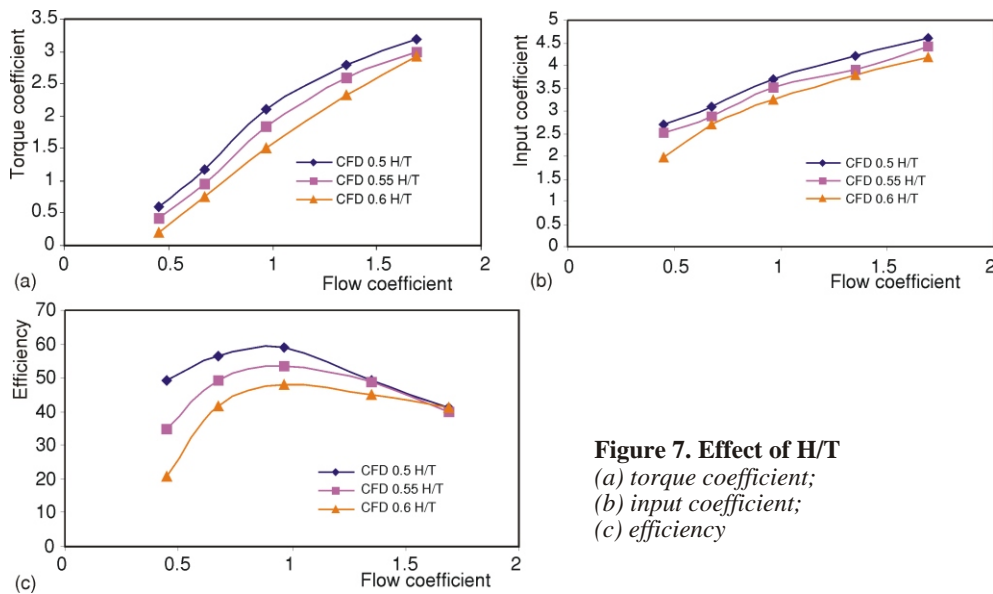


**Figure 7. Effect of H/T**  
(a) torque coefficient;  
(b) input coefficient;  
(c) efficiency

#### *Computed flow behaviour due to effect of guide vane shape*

In order to investigate the effect of H/T in the flow field, velocity contours have been plotted at various blade heights hub-mid-span-tip for the cases of 0.5 and 0.55 H/T turbine at the designed condition of flow coefficients of 1.0 and rotational speed of 350 rpm is shown in fig. 8a-f, respectively. The flow coefficients have been chosen to investigate the flow in design ( $\phi = 1.0$ ) condition. From the fig. 8d-f, it is observed that the flow entering in to the downstream guide vane is being separated by leading edge of downstream guide vanes, causing large recirculation zone for the case of 0.55 H/T turbine. But, by using the 0.5 H/T turbine, fig. 8a-c, the recirculation has reduced slightly from hub to med region,

but, higher flow separation still occur at the tip region. The flow insight gives enough reason for the improvement in torque developed by the 0.5 H/T turbine at the flow coefficient of 1.0, fig. 7a, and also it gives us clear picture in where flow separations are occur in our models.

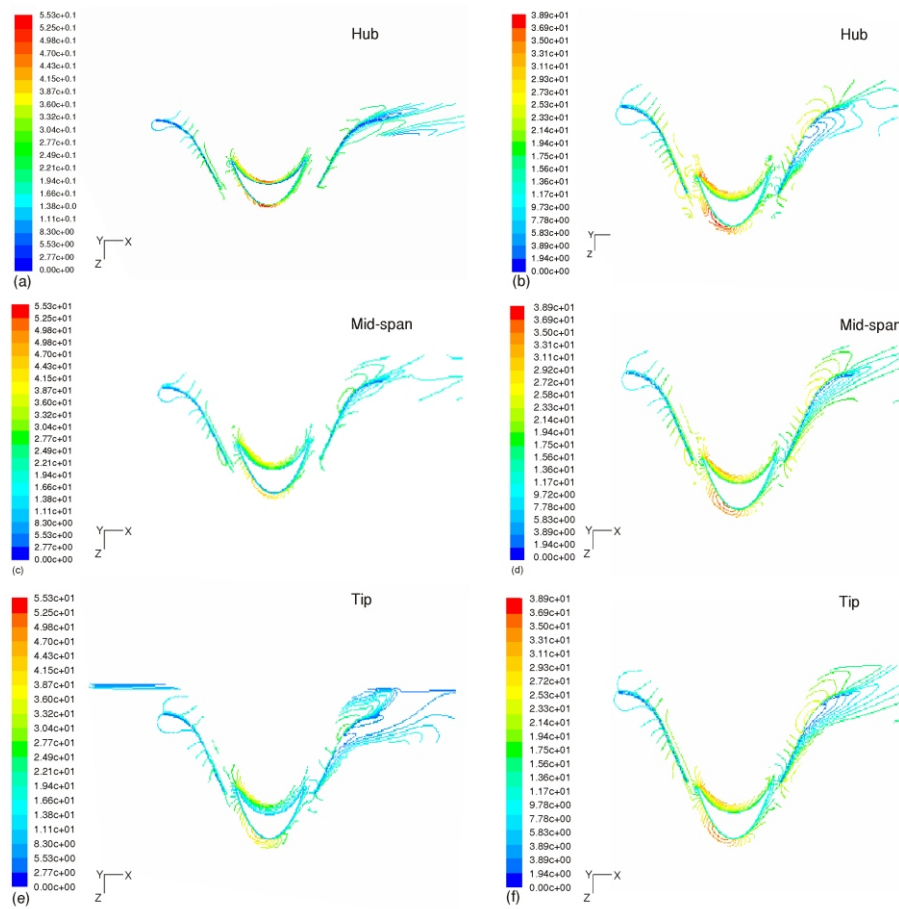


Figure 8a-f. Velocity contours at various blade heights at  $\phi = 1, 0.5$  left (0.5 H/T), right (0.55 H/T)

## Conclusions

The present computational model has been validated with experimental results with reasonable accuracy and found well suitable for further design analysis. It is found that  $k-\varepsilon$  turbulence model can predict the performance of turbine well in the low rotational

speed of turbine. The performance curves of the impulse turbine with various H/T have been arrived numerically. It is evident that the downstream guide vanes are causing the flow separation; hence, the shape of the upstream and downstream should be investigated. The CFD analysis shows that the turbine with 0.5 H/T has better performance compared to 0.55 and 0.6 H/T turbine.

### Nomenclature

$b$  – height of blade, [mm]  
 $l_r$  – chord length of rotor blade, [mm]  
 $r_R$  – mid span radius, [mm]  
 $U_R$  – circumferential velocity at  $r_R$ , [ms<sup>-1</sup>]  
 $v_a$  – axial flow velocity, [ms<sup>-1</sup>]  
 $z$  – number of rotor blades, [–]

### Greek letters

$\phi$  – flow coefficient, [–]  
 $\rho$  – density of air, [kgm<sup>-3</sup>]

### Acknowledgments

The authors would like to acknowledge the financial support given by Wave Energy Research Team and also Department of Mechanical and Aeronautical Engineering, University of Limerick.

### References

- [1] Duckers, L., Wave Energy (Chapter 8), in: *Renewable Energy – Power for a Sustainable Future* (Ed. G. Boyle), Oxford University Press, Oxford, UK, 1996, pp. 315-352
- [2] Gato, L., Warfield, V., Performance of a High-Solidity Wells Turbine for an OWC Wave Power Plant, *Proceedings*, 1993 Euro Wave Energy Symposium, NEL, UK, 1994, pp. 181-190
- [3] Inoue, M., Kaneko, K., Setoguchi, T., Saruwatari, T., Studies on the Wells Turbine for Wave Power Generator (Turbine Characteristics and Design Parameters for Irregular Waves). *JSME Int. J. Ser. 2*, 31 (1988), 4, pp. 676-682
- [4] Raghuanathan, S., Tan, C. P., Performance of the Wells Turbine at Starting, *J. Energy*, 6 (1982), 6, pp. 430-431
- [5] Kim, T. W., Kaneko, K., Setoguchi, T., Inoue, M., Aerodynamic Performance of an Impulse Turbine with Self-Pitch-Controlled Guide Vanes for Wave Power Generator, *Proceedings*, 1<sup>st</sup> KSME-JSME Thermal and Fluid Engg. Conference, Seoul, 1988, Vol. 2, pp. 133-137
- [6] Kim, T. W., Kaneko, K., Setoguchi, T., Matsuki, E., Inoue, M., Impulse Turbine with Self-Pitch-Controlled Guide Vanes for Wave Power Generator (Effects of Rotor Blade Profile and Sweep Angle), *Proceedings*, 2<sup>nd</sup> KSME-JSME Thermal and Fluid Engg. Conference, Seoul, 1990, Vol. 1, pp. 277-281

- [7] Setoguchi, T., Kaneko, K., Maeda, H., Kim, T. W., Inouse, M., Impulse Turbine with Self-Pitch-Controlled Guide Vanes for Wave Power Conversion: Performance of Mono-Vane Type, *Int. J. Offshore and Polar Engg.*, 3 (1993), 1, pp. 73-78
- [8] Setoguchi, T., Kaneko, K., Maeda, H., Kim, T. W., Inoue, M., Impulse Turbine with Self-Pitch-Controlled Tandem Guide Vanes for Wave Power Conversion. *Proceedings*, 3<sup>rd</sup> International Offshore and Polar Engineering Conference, Singapore, 1993, Vol. 1, pp. 161-166
- [9] Maeda, H., Setoguchi, T., Kaneko, K., Kim, T. W., Inoue, M., The Effect of Turbine Geometry on the Performance of Impulse Turbine with Self-Pitch-Controlled Guide Vanes for Wave Power Conversion, *Proceedings*, 4<sup>th</sup> International Offshore and Polar Engineering Conference, Osaka, Japan, 1994, Vol. 1, pp. 378-382
- [10] Setoguchi, T., Kaneko, K., Maeda, H., Kim, T. W., Inouse, M., Impulse Turbine with Self-Pitch-Controlled Tandem Guide Vanes for Wave Power Conversion, *Int. J. Offshore and Polar Engg.*, 4 (1994), 1, pp. 76-80
- [11] Maeda, H., Setoguchi, T., Kaneko, K., Kim, T. W., Inoue, M., Effect of Turbine Geometry on the Performance of Impulse Turbine with Self-Pitch-Controlled Guide Vanes for Wave Power Conversion, *Int. J. Offshore and Polar Engg.*, 5 (1995), 1, pp. 72-74
- [12] Setoguchi, T., Kaneko, K., Taniyama, H., Maeda, H., Inoue, M., Impulse Turbine with Self-Pitch-Controlled Guide Vanes for Wave Power Conversion: Guide Vanes Connected by Links. *Int. J. Offshore and Polar Engg.*, 6 (1996), 1, pp. 76-80
- [13] Kim, T. S., Lee, H. G., Ill-Kyoo Park, Lee, Y. W., Kinoue, Y., Setoguchi, T., Numerical Analysis of Impulse Turbine for Wave Energy Conversion. *Proceedings*, 10<sup>th</sup> International Offshore and Polar Engineering Conference, Sietle, USA, 2000, Vol. 1, pp. 413-419
- [14] Thakker, A., Dhanasekaran, T. S., Experimental and Computational Analysis on Guide Vane Losses of Impulse Turbine for Wave Energy Conversion, *Renewable Energy*, 30 (2005), 9, pp. 1359-1372
- [15] Raghunathan, S., Setoguchi, T., Kaneko, K., Aerodynamics of Monoplane Wells Turbine – A Review, *Int. J. Offshore and Polar Engg. ISOPE*, 4 (1994), 1, pp. 68-75
- [16] Tagori, R., Arakawa, C., Suzuki, M., Estimation of Prototype Performance and Optimum Design of Wells Turbine, Research in Natural Energy, SPEY 20 (The Ministry of Education, Science and Culture, Japan), 1987, pp. 127-132
- [17] Raghunathan, S., The Wells Air Turbine for Wave Energy Conversion, *Prog. Aerospace Sci.* 31 (1995), 4, pp. 335-386
- [18] Thakker, A., Dhanasekaran, T. S., Computed Effects of Tip Clearance on Performance of Impulse Turbine for Wave Energy Conversion, *Renewable Energy*, 29 (2003), 4, pp. 529-547
- [19] Hourigan, F., Dhanasekaran, T. S., Hemry, M. El., Usmani, Z., Rayan, J., Design and Performance Analysis of Impulse Turbine for a Wave Energy Power Plant, *International Journal of Energy Research*, 29 (2004), 1, pp. 13-36
- [20] Setoguchi, T., Santhakumar, S., Maeda, H., Takao, M., Kaneko, K., A Review of Impulse Turbine for Wave Power Energy Conversion, *Renewable Energy*, 23 (2001), 2, pp. 261-292
- [21] \*\*\*, FLUENT Users Manuals 2003, Fluent Inc.

Authors' address:

*A. Thakker*

Department of Mechanical and Aeronautical Engineering  
University of Limerick, Ireland

*M. A. Elhemry*

Wave Energy Research Team (WERT)  
Department of Mechanical and Aeronautical Engineering  
University of Limerick, Ireland

Corresponding author A. Thakker

E-mail: [Ajit.Thakker@ul.ie](mailto:Ajit.Thakker@ul.ie)

Paper submitted: November 7, 2006

Paper revised: July 16, 2007

Paper accepted: October 30, 2007